The potential of Pléiades images with high angle of incidence for reconstructing the coastal cliff face in Normandy

Pauline Letortu, Marion Jaud, Claire Théry, Jean Nabucet, Roza Taouki, Sophie Passot, Emmanuel Augereau

The potential of Pléiades images with high angle of incidence for reconstructing the coastal cliff face in Normandy (France)

Pauline Letortu[a*], Marion Jaud[a,b], Claire Théry[a], Jean Nabucet[c], Roza Taouki[a], Sophie Passot[d], Emmanuel Augereau[a]

[a]*University of Bretagne Occidentale, IUEM, CNRS, UMR 6554 – LETG, Technopôle Brest-Iroise, rue Dumont d'Urville, Plouzané, 29280, France, pauline.letortu@univ-brest.fr, claire_thery1@hotmail.fr, Roza.Taouki@ensg.eu, emmanuel.augereau@univ-brest.fr*

[b]*University of Bretagne Occidentale, IUEM, CNRS, UMS 3113 – IUEM, Technopôle Brest-Iroise, Rue Dumont d'Urville, Plouzané, 29280, France, marion.jaud@univ-brest.fr*

[c]*University of Rennes 2, CNRS, UMR 6554 – LETG, Place du Recteur Henri Le Moal, Rennes, 35000, France, jean.nabucet@uhb.fr*

[d]*Université Claude Bernard Lyon 1, UMR 5276 - Laboratoire de Géologie de Lyon: Terre, Planètes, Environnement, ENS Lyon, Villeurbanne, 69622, France, sophie.passot@univ-lyon1.fr*

[e]*University of Bretagne Occidentale, IUEM, CNRS, UMR 6538 – IUEM, Technopôle Brest-Iroise, Rue Dumont d'Urville, Plouzané, 29280, France*

*Corresponding author. Tel.: +33 290915588, pauline.letortu@univ-brest.fr

Abstract

To monitor chalk cliff face along the Normandy coast (NW France) which is prone to erosion, we tested the potential of cliff face 3D reconstruction using pairs of images with high angle of incidence at different dates from the agile Pléiades satellites. The verticality aspect of the cliff face brings difficulties in the 3D reconstruction process. Furthermore, the studied area is challenging mainly because the cliff face is north-oriented (shadow). Pléiades images were acquired over several days (multi-date stereoscopic method) with requested incidence angles until 40°. 3D reconstructions of the cliff face were compared using two software: ASP® and ERDAS IMAGINE®. Our results are twofold. Firstly, despite ASP® provides denser point clouds than ERDAS IMAGINE® (an average of 1.60 points/m² from 40° incidence angle stereoscopic pairs on the whole cliff face of Varengeville-sur-Mer against 0.77 points/m² respectively), ERDAS IMAGINE® provides more reliable point clouds than ASP® (precision assessment on the Varengeville-sur-Mer cliff face of 0.31 m ± 2.53 and 0.39 m ± 4.24 respectively), with a better spatial distribution over the cliff face and a better representation of the cliff face shape. Secondly, the quality of 3D reconstructions depends mostly on the amount of noise from raw images and on the shadow intensity on the cliff face (radiometric quality of images).

Keywords

Pléiades imagery; high incidence angle images; cliff face erosion; 3D reconstruction; Normandy

1. Introduction

Coastal areas have high density populations due to rich resources and good social and recreational infrastructures. This trend is likely to increase with time but with spatial differences (Neumann et al., 2015). About 52% of the global shoreline is made of cliff coasts that can only retreat (Young and Carilli, 2019). The erosion of these coasts could be dramatic, with occasional massive falls which can threaten people, buildings, utilities and infrastructure located near the coastline (Lim et al., 2005; Naylor et al., 2010; Moses and Robinson, 2011; Kennedy et al., 2014; Letortu et al., 2019). Traditionally, the study of cliff coasts involves quantifying the retreat rates of the cliff top (m/year) with 2D data. This diachronic approach (over several decades) is mainly based on vertical aerial photographs more recently using

airborne LIDAR data over a significant spatial scale (several tens to hundreds of kilometers) at multi-year intervals (Young, 2018). These average annual retreat rates poorly reflect the erosive dynamics of cliffs, which are characterized by dead time (marine, subaerial, anthropogenic agents weaken the cliff without eroding it) and high points (sudden falls causing cliff retreat). Subsequently, the fall deposit is evacuated by marine action and erosion continues its action on the new cliff face. Scientists have identified the conditions for a better understanding of the regressive dynamics of cliffs (retreat rates, rhythms of evolution, triggering factors of failure). It is necessary to collect 1) 3D data of the cliff face (from the foot to the top of the cliff) to observe all erosion events (2) at high spatial resolution (inframetric) (3) at very high temporal frequency (from seasonal to daily surveys) and (4) over large-scale areas (hydro-sedimentary cell scale for relevant coastal management).

While the terrestrial laser scanning and the UAV photogrammetry or terrestrial photogrammetry can meet the first three conditions, the low spatial representativeness of the results is a major constraint (James and Robson, 2012; Letortu et al., 2018; Westoby et al., 2018). The boat-based mobile laser scanning data bring together three of the conditions but the cost and the necessary technical know-how limit the temporal frequency of the surveys (Michoud et al., 2014). Moreover, these methods can be very expensive and need staff on the field. Images from Pléiades satellites launched in 2011 and 2012 could be adequate because these satellites are very agile (they can reach a viewing angle of up to 47° to image the cliff face), the data are at very high spatial resolution (around 0.70 m ground sampling distance at nadir for panchromatic images), with a daily revisit frequency and a swath width of 20 km at nadir (ASTRIUM, 2012; Boissin et al., 2012). The images acquired from a pushbroom scanner may be free (under certain conditions) for research institutes and do not require specific fieldwork.

In a context of coastal morphology mapping, satellite imagery has long been used for large-scale 2D studies, enabling to map shoreline/coastline position and to analyze its evolution (e.g. White and El Asmar, 1999; Boak and Turner, 2005; Gardel and Gratiot, 2006). The development of high-resolution agile satellites has opened up new perspectives, especially for 3D reconstruction. Many articles have used Pléiades stereoscopic or tri-stereoscopic acquisitions to answer various scientific questions (e.g. de Franchis et al., 2014; Stumpf et al., 2014; Poli et al., 2015) including in coastal environments (AIRBUS, 2015; Collin et al., 2018; Almeida et al., 2019). But, to our knowledge, Pléiades satellite images have never been used in the context of cliff face monitoring which is challenging because it raises four questions:

- How to collect Pléiades images on a vertical cliff face?
- How to process these high angle of incidence images?
- What is the relevance of this data for cliff face 3D reconstruction (sufficient point density on the cliff face to observe structural discontinuities)?
- What are the favorable acquisition parameters and site characteristics for cliff face surveys (angle of incidence, season, orientation of the coastline, color of the cliff face)?

For this study, images were acquired along the Norman coastal cliffs (Seine-Maritime), from Quiberville to Berneval-le-Grand (20 km, north-oriented cliff face) because the risk of erosion is significant. The fast retreat rate of chalk cliffs has reached urban areas and impacted the local use of the beach. Some areas are under expropriation procedures to protect populations (Dieppe) and a fatality occurred in August 2015 in Varengeville-sur-Mer where a shell fisherman died after being buried by tons of rock due to chalk cliff fall. One of the challenges in coastal management is to predict the coastal evolution in order to protect people living in this environment. This challenge can be achieved using relevant, homogeneous and long-term data including these provided by Pléiades imagery.

The standard stereoscopic or tri-stereoscopic acquisition which consists, within the same pass of the satellite on its meridian orbit, of acquiring two or three images over the area of interest (front, nadir and back images) is proved unsuitable in our case because of the orientation of the cliff face: the backward viewing image would capture the plateau but not the cliff face making 3D reconstruction impossible. Furthermore, the studied cliff face being a sub-vertical object, a high angle of incidence should be favorable. Thus, we imagined an original acquisition procedure: as the orbital pass position changes daily, a multi-date survey over several consecutive days, with mono-acquisition and a high angle of incidence (across-track), was performed to observe the area at various viewing angles. In order to assess the impact of the angle of incidence, two sets of images were simultaneously requested: one with a pitch imaging angle of 40° and the second one with a pitch imaging angle between 0° and 10°.
First, the study area will be described, followed by the methods of acquisition and data processing of images with a high angle of incidence. In a third step, the results of our exploratory research on the relevance of Pléiades data for reconstructing the Norman cliff face and the favorable acquisition parameters and site characteristics will be presented and discussed. Conclusions will be drawn in the final section.

2. Study area

The study area is located in north-western France (01°00'E; 49°55'N), in Normandy (Seine-Maritime), along the Channel. Climatically, the area belongs to the western part of Europe which is particularly exposed to the influences of oceanic low pressures, and thus, to the types of disturbed weather that dominate approximately 2/3 of the year (Pédelaborde, 1958; Trzpit, 1970). Geologically, it belongs to the northeastern part of the Parisian Basin (sedimentary), where the Pays de Caux plateau abruptly ends in subvertical coastal cliffs. Cliffs are made of Upper Cretaceous chalk with flints (Pomerol et al., 1987; Mortimore et al., 2004). The altitude range of the cliffs is between 20 m to 100 m with an increase from south-west to north-east, and locally cut by valleys. As shown in Figure 1, these cliffs are mainly white in color, but the sub-vertical cliffs are darkened (brown color) by a bed of clay and sand sediment of the Tertiary Period (Paleogene) between Sainte-Marguerite-sur-Mer and Dieppe, and elsewhere by clay-flint formations above the chalk strata. The average tidal range is 8 m (macrotidal environment). At low tide the foreshore is characterized by a wide shore platform slightly inclined to the sea with a gravel barrier near the cliff foot contact.

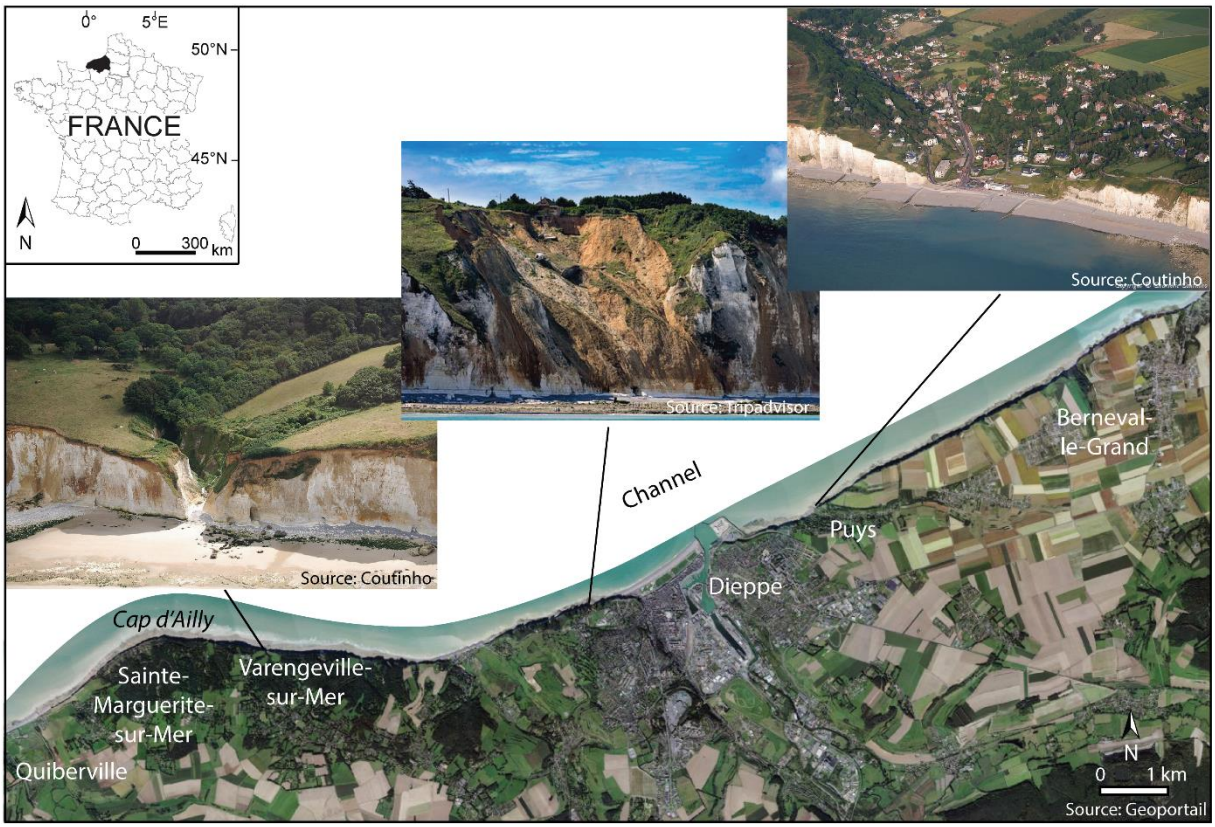

Figure 1 : Presentation of the study area from Quiberville to Berneval-le-Grand (Seine-Maritime, Normandy)

Along the studied coastline (between Quiberville and Berneval-le-Grand, 20-km long), the lithology of the cliffs from Sainte-Marguerite-sur-Mer to Dieppe is composed of Santonian and Campanian chalk and covered by Paleogene strata. The lithology is prone to erosion with the highest annual retreat rate (0.23 m/year) in comparison with average county retreat rate (0.15 m/year between Cap d'Antifer and Le Tréport, 1966-2008 (Letortu et al., 2014)). Between Dieppe and Berneval-le-Grand (Turonian and Coniacian chalk stages), the retreat rate is lower (0.12 m/year). The modalities of erosion are varied with falls of a few m^3 to hundreds of thousands of m^3 but they are ubiquitous along the cliff line.

The study area is challenging for the acquisition of these satellite images because (1) the SW/NE orientation of the coastline complicates the image acquisition while the Pléiades orbit is meridian; (2) the cliff face is north-oriented, so in the cast shadow during the satellite passing time, even in summer; (3) the weather conditions are often cloudy and rainy in the area because it is located in mid-latitudes where disturbed weather dominates; (4) a high tidal range limits the acquisition periods because the whole cliff face is needed.

For the 3D reconstruction, the diversity of cliff types along the 20 km cliff line is also challenging. To assess the quality of reconstructions in function of the site characteristics, four areas of interest (AOIs) were selected: Sainte-Marguerite-sur-Mer, Varengeville-sur-Mer, Dieppe and Puys (Table 1, Figure 2). The whitest cliff faces are located at Puys. The cliff face colors at Sainte-Marguerite-sur-Mer, Varengeville-sur-Mer and Dieppe are from brown to light gray. The shore platform is gray or beige and mainly rocky with gravel accumulation except at Puys, where there are no gravel accumulations. Sainte-Marguerite-sur-Mer and Varengeville-sur-Mer have the lowest cliff height (from 20 to 40 m), with the gentlest cliff face slope at Sainte-Marguerite-sur-Mer (70°). Sainte-Marguerite-sur-Mer and Puys have a sublinear coastline

(average depth of incisions from 10 to 20 m) whereas Varengeville-sur-Mer and Dieppe have a jagged coastline (incisions from 75 to 115 m-deep) (Figure 2).

Area of interest (AOI)	Sainte-Marguerite-sur-Mer (00°56'37"E; 49°54'42"N)	Varengeville-sur-Mer (01°00'22"E; 49°55'01"N)	Dieppe (01°03'33"E; 49°55'27"N)	Puys (01°07'26"E; 49°56'38"N)
Cliff face color	Ochre and light gray	Brown and light gray	Brown and light gray	Light gray
Shore platform color	Dark gray	Beige	Dark gray	Light gray
Type of platform	Rocky and gravel accumulation	Rocky and gravel accumulation	Rocky and gravel accumulation	Rocky
Average cliff height (m)	20-50	30-40	60	70
Average cliff face slope (°)	70	70-90	80-85	80-90
Orientation of cliff face	NW	NNE	NNW	NNW
Average depth of incision* (m)	10	115	75	20

Table 1: Main characteristics of the AOI sites (*the depth of incision is the length from the headland to the trough (perpendicular to the coastline))

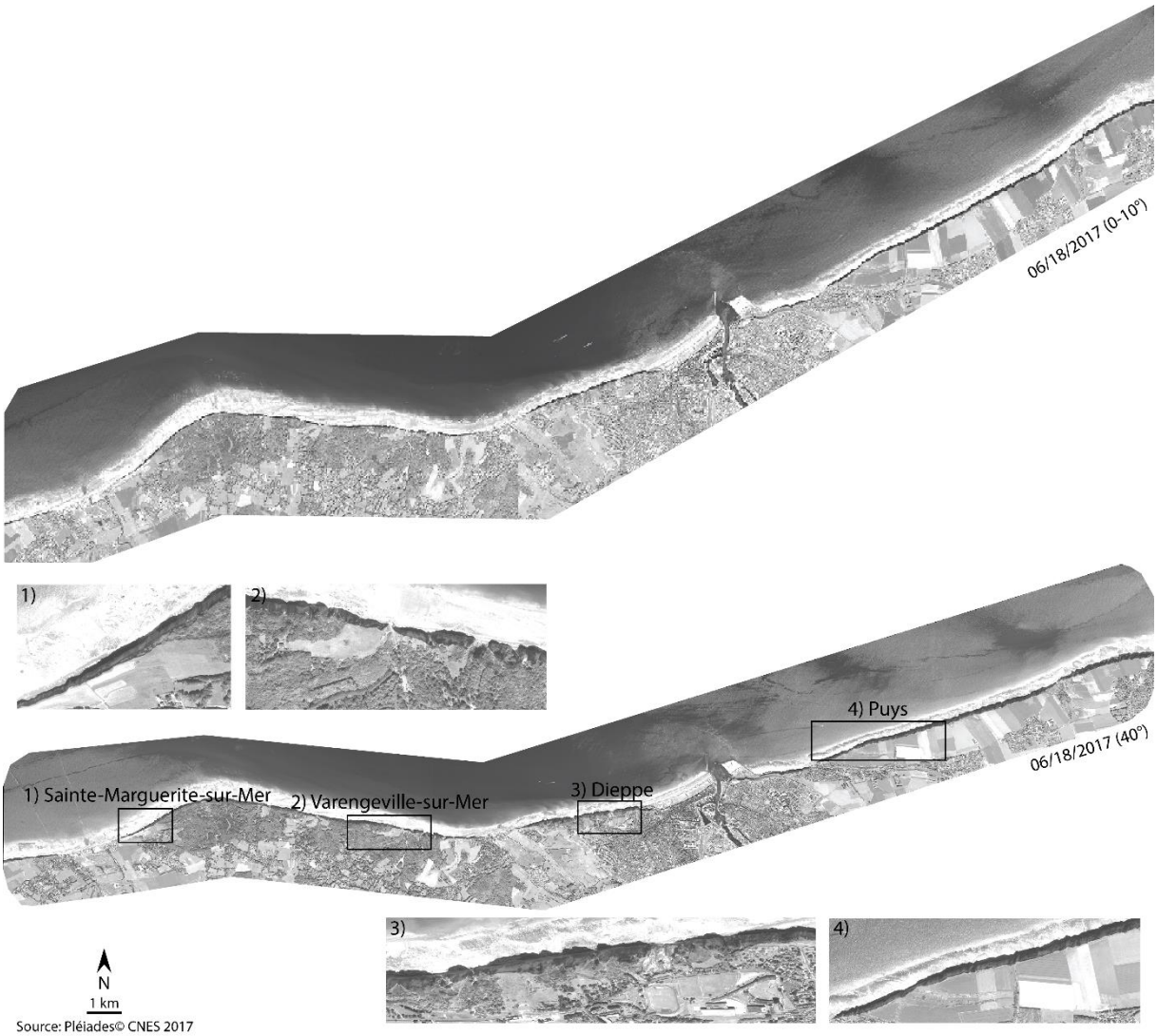

Figure 2: Images acquired on 06/18/2017 with both requested incidence angles and the location of AOIs

3. Data collection and processing

3.1. Acquisition strategy

The high angle of incidence needed for the images of the multi-date survey requires the satellite position at the time of acquisition to be above the Channel or the United Kingdom (Figure 3). This means that cloud cover must be from zero to low over large areas, around 11:25 UTC (satellite pass time).

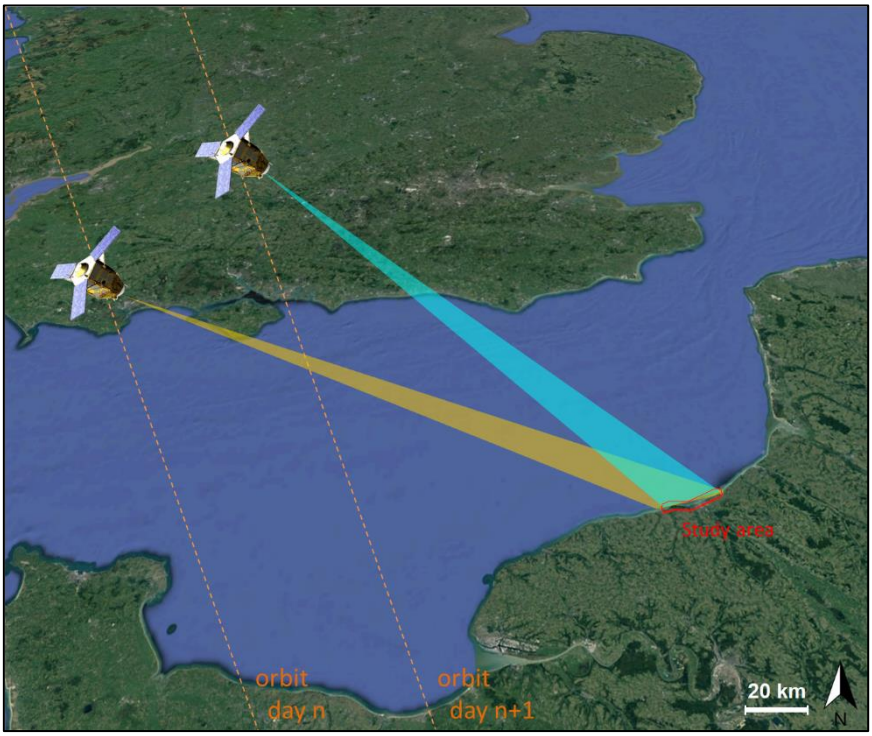

Figure 3: Principle of the multi-date survey used in this study

In this configuration, the acquisition is considered challenging by the image supplier due to the high incidence angle, repetitiveness and short periods of time when the site is accessible under good conditions (zero or low cloud cover (between 0 and 10%) and during low tide if possible).

3.2. Acquired images and stereo-pairs

In order to follow the evolution of the studied cliffs, different periods were chosen for Pléiades image acquisition:

- Fall 2016: 4 stereoscopic pairs;
- Summer 2017: 5 stereoscopic pairs (Figure 2);
- Winter 2017/2018: 5 stereoscopic pairs.

The angle of incidence is different from the viewing angle due to the sphericity of the Earth. To limit the differences induced by the geometric configuration of the images, we chose to perform 3D reconstruction from images acquired with similar incidence angles (either 40° or 0-10°). The images acquired (Table 2) used in this paper are panchromatic ones, as spatial resolution is finer (0.7 m) than multispectral images (2.8 m). However, due to the geometry of acquisition, the ground sampling distance is variable from one day to another, varying for example from 0.27 m to 1.83 m for images at 40° of incidence.

Date	Hour (UTC)	Name of satellite	Requested incidence angle	Weather	Pitch viewing angle (°)	Roll viewing angle (°)	Pitch incidence angle (°)	Roll incidence angle (°)	Oblique distance between the satellite and the cliff (m)
10/05/2016	11:29	1B	0-10	Sunny	2.25	29.16	12,96	-3.01	707856
10/06/2016	11:21	1A	0-10	Cloudy	4.78	20.75	-11.50	-21.13	727351
10/08/2016	11:06	1A	0-10	Sunny	-0.7	0.9	0.74	-1.16	694160
10/31/2016	11:29	1B	0-10	Sunny	-1.06	29.28	-9.49	-31.98	700857
06/10/2017	11:21	1B	0-10	Sunny	9.65	20.6	-16.56	-19.65	743652
06/15/2017	11:33	1B	0-10	Sunny	1.01	32.83	-11.75	-35.9	703506
06/18/2017	11:10	1A	0-10	Sunny	3.07	6.47	-4.6	-5.39	698687
07/06/2017	11:21	1B	0-10	Cloudy	9.13	20.45	-15.95	-19.64	742090
07/21/2017	11:06	1A	0-10	Sunny	9.71	0.17	-10.4	2.2	916552
12/01/2017	11:32	1A	0-10	Cloudy	30.47	31.29	-11.75	-35.86	884638
12/16/2017	11:17	1B	0-10	Cloudy	9.71	15.72	-14.78	-14.35	759203
01/24/2018	11:17	1A	0-10	Cloudy	-0.66	16.09	-3.88	-17.54	731573
02/12/2018	11:20	1A	0-10	Cloudy	9.15	20.34	-15.93	-19.51	742410
02/17/2018	11:32	1A	0-10	Sunny	5.91	32.44	-18.71	-33.79	720932
10/05/2016	11:27	1B	40	Sunny	40.65	26.65	-50.56	-15.94	1023748
10/06/2016	11:20	1A	40	Cloudy	30.39	19.35	-37.59	-11.93	884387
10/08/2016	11:05	1A	40	Cloudy	34,15	0.7	-37.55	10.79	850050
10/31/2016	11:28	1B	40	Misty	30.39	27.7	-40.49	-21.52	878726
06/10/2017	11:20	1B	40	Sunny	40.69	18.35	-48.5	-6.23	1026143
06/15/2017	11:31	1B	40	Sunny	30.48	31.32	-42.09	-25.81	884838
06/18/2017	11:08	1A	40	Sunny	37.32	3.83	-41.92	7.65	890433
07/06/2017	11:20	1B	40	Sunny	30.46	19.22	-37.62	-11.77	885380
07/21/2017	11:05	1A	40	Sunny with scattered clouds	39.24	1.42	-43.56	13.63	704437
12/01/2017	11:31	1A	40	Cloudy	-1.03	32.79	-42.08	-25.74	703402
12/16/2017	11:17	1B	40	Cloudy	30.43	14.5	-36.34	-6.6	896286
01/24/2018	11:16	1A	40	Cloudy	30.48	14.46	-36.38	-6.57	896897
02/12/2018	11:20	1A	40	Cloudy	30.46	19.11	-37.59	-11.67	885643
02/17/2018	11:30	1A	40	Sunny	36.03	30.63	-47.2	-22.92	954538

Table 2: Characteristics of acquired Pléiades images

For the 3D reconstruction of the cliff face, the 0-10° and 40° images were examined according to three criteria to select the stereoscopic pairs which appeared relevant to process:

- The absence of rock falls between both images: Thus, a study of falls on the AOIs between 2016 and 2018 identified one fall at Varengeville-sur-Mer on 10/23/2017, two falls at Sainte-Marguerite-sur-Mer (one between 07/21/2017 and 12/12/2017, the other between 07/21/2017 and 12/01/2018), one fall at Puys (between 01/24/2018 and 02/12/2018). It is possible that some falls were missed, therefore it was decided that the acquisition period for stereoscopic image pairs should not exceed 2 months;
- Good image quality: A clear sky is required between the satellite and the study area to have a cloud-free imagery (Berthier et al., 2014), thus a satisfactory radiometric quality. This statement is also true for the cliff shadow. In our study area, a good radiometric quality (values of the pixels vary from 0 to 4095 for 12 bit images) is between 134 and 827 for the mean value and between 177 and 1543 for the standard deviation. Meteorology and the size of the shadow on the cliff face have been grouped together under the parameter "visual image evaluation". Only images with good visual image evaluation were retained.
- The “flattening” coefficient of the pixels must be limited: where pixel flattening coefficient=Image resolution (x)/Image resolution (y). In our study, flattening coefficient has to be between 0.22 and 2.23 to facilitate feature recognition between images. Not surprisingly,

the flattening of the pixels is much less marked at 0-10° than at 40° (on average 0.92 at 0-10°and 0.55 at 40°).

Taking into account these three criteria, 23 image pairs were tested (Table 3).

Date of stereoscopic pairs		Incidence angles (°)
06/10/2017	06/15/2017	0-10
06/15/2017	07/06/2017	0-10
12/01/2017	12/16/2017	0-10
01/24/2018	02/12/2018	0-10
01/24/2018	02/17/2018	0-10
02/12/2018	02/17/2018	0-10
10/05/2016	10/08/2016	40
10/05/2016	10/31/2016	40
10/08/2016	10/31/2016	40
06/10/2017	06/15/2017	40
06/10/2017	06/18/2017	40
06/10/2017	07/06/2017	40
06/15/2017	06/18/2017	40
06/15/2017	07/06/2017	40
06/15/2017	07/21/2017	40
06/18/2017	07/06/2017	40
06/18/2017	07/21/2017	40
07/06/2017	07/21/2017	40
12/01/2017	12/16/2017	40
12/01/2017	01/24/2018	40
01/24/2018	02/12/2018	40
01/24/2018	02/17/2018	40
02/12/2018	02/17/2018	40

Table 3: Stereoscopic pairs used for data processing

3.3. Data processing

Usually, different software (commercial and open-source) can be used for 3D reconstruction but, in our case, the unusual configuration of images may restrict the choice of suitable software.

In this study, an open-source (ASP® 3.5.1) and a commercial software (ERDAS IMAGINE ®) were used. ERDAS IMAGINE® is a commercial software suite for the creation, visualization, geocorrection, reprojection and compression of geospatial data. ASP® (Ames Stereo Pipelines, NASA) is a suite of free and open-source automated geodesy and stereogrammetry tools (Shean et al., 2016) notably developed for satellite imagery with very detailed documentation (NASA, 2019, https://ti.arc.nasa.gov/tech/asr/groups/intelligent-robotics/ngt/stereo/#Documentation).

Internal and external parameters of the pushbroom sensor are provided with each image. They are empirically described using rational polynomial camera model. Images are provided with Rational Polynomial Coefficients (RPCs), approximating functions which describe the relationship between image space and object space (de Franchis et al., 2014). RPCs are accurate only within a specified validity zone and can reveal inconsistencies for large scenes and/or multi-temporal acquisitions (Rupnik et al., 2016). Both ERDAS IMAGINE® and ASP® use RPC sensor model to perform orthorectification and georectification. For some processing chains, RPCs are computed or affined using Ground Control Points (GCPs) collected

throughout the area (Salvini et al., 2004; Kotov et al., 2017). In our case, no GCPs were used and the RPC-based sensor orientation was only refined using tie points identified on both images of the pair.

In ERDAS IMAGINE®, automatic tie point detection provided poor results probably due to high incidence angles and multi-date images. To improve detection, we manually pointed tie points on each image. A minimum of 25 points was chosen (optimal threshold defined after trials between availability of relevant tie points and quality of Root Mean Square Error (RMSE)). These points are preferably identifiable and unchangeable elements on flat areas, where distortions are limited (middle of a crossroads rather than a house roof). In addition, tie points are mainly located near the coast in order to minimize correlation errors over this area of interest. A polynomial model is considered satisfactory when all the points have a RMSE inferior to 0.5 pixels (Vanderstraete et al., 2003). When the RMSE of the triangulation ratio was greater than 0.5 pixels or when the uncertainty threshold was greater than 4 meters for a tie point, it was systematically removed and replaced by a better point. In ASP®, we skipped this step because co-registration using a rigid-body transformation can accomplish similar results with reduced processing time (Shean et al., 2016).

Epipolar images are then computed to perform stereo-matching in both software (Normalized Cross Correlation algorithm in ERDAS IMAGINE®, More Global Matching (MGM) one in ASP®). This stereo-matching step consists of cross-correlation to identify pixel correspondences between the left and right epipolar images. Given characteristic variations of the stereoscopic pairs (multi-date), it is difficult to standardize the processing parameters within the software and between software. As the areas of interest correspond to steep slopes, we used small correlation windows (7*7 pixels, 9*9 pixels). The small size of the windows may introduce more false matches or noise (NASA, 2019). Because of the shadow on the cliff face, the “low contrast” parameter was activated in ERDAS IMAGINE® during the image matching to force it to find tie points in this area. In ASP®, the MGM algorithm was used to decrease high frequency artifacts in low texture areas in order to find more corresponding pixels between both images.

Sub-pixel refinement was used in ERDAS IMAGINE® (Least Square Refinement) whereas it was not used in ASP® in order to reduce processing time (Shean et al., 2016) without altering quality of our results.

In ASP®, we used post filtering to filter disparity (artifacts) with three filters: median-filter-size (3 pixels), texture-smooth-size (11 pixels) and texture-smooth-scale (0.15 pixels).

Finally, a 3D position can be computed for each pair of corresponding pixels. The software also generate a DEM, but considering the verticality of the cliff face, we only exported the 3D point cloud.

The point clouds are then post-processed with CloudCompare®, an open-source software, to manually filter artifacts in the point cloud.

To assess the impact of the study site characteristics and of the acquisition parameters, the parameterization of both software was not changed from one stereoscopic pair to another or from one AOI to another.

4. Results and discussion

4.1. Comparison of the results provided by the different processing

4.1.1. Point density

In order to have a relevant cliff face monitoring, it is necessary that the whole cliff face is sampled during 3D reconstruction with sufficient resolution to observe the structural discontinuities of the cliff face. The average density of the point clouds corresponding to the Varengeville-sur-Mer cliff face is calculated (Table 4). The point density is much higher for 3D

reconstructions made with ASP® than ERDAS IMAGINE® (respectively, 1.86 points/m² versus 0.24 points/m² on the whole cliff face for 0-10° of incidence angle and 1.60 points/m² versus 0.77 points/m² for 40° of incidence angle). Regardless of the angle of the images and the used software, the cliff foot is the least densely reconstructed part (0.74 points/m² with ASP® and 0.04 points/m² with ERDAS IMAGINE® for a pair of images at 0-10°) while the most reconstructed part is the cliff top (1.37 points/m² with ASP® and 0.89 points/m² with ERDAS IMAGINE® for a pair of images at 40°). This point density difference might be due to the correlation step using different algorithms.

Location on the cliff face	Requested incidence angles used for 3D reconstruction	Average point density (number of points/m²) with ASP®	Average point density (number of points/m²) with ERDAS IMAGINE®
Cliff top	0-10°	1.87	0.15
	40°	1.37	0.89
Middle of the cliff face	0-10°	1.64	0.13
	40°	1.45	0.67
Cliff foot	0-10°	0.74	0.04
	40°	1.03	0.25
Whole cliff face	0-10°	1.86	0.24
	40°	1.60	0.77

Table 4: Average density of the point clouds in Varengeville-sur-Mer in function of the cliff face part and the used software

4.1.2. Point distribution

The point distribution of the 3D reconstructions obtained on the cliff face with both software is different (Figure 4). Although the point cloud obtained with ASP® is denser than that obtained with ERDAS IMAGINE®, the shape of the cliff is more realistic with ERDAS IMAGINE® (see dotted black frames in Figure 4).

With ASP®, there are very few artifacts on the plateau and on the platform. They are mainly located on edges of the point cloud and at shadow/sunlit contact (white dotted circles depict areas where the contact is located about 20 m from the foot of the cliff (Figure 4)). At this latter area, artifacts have the shape of a stair step.

For ERDAS, there are spike-shaped artifacts on the plateau but also on the platform because the optimization of processing parameters is focused on the cliff face and is not suitable for the whole area. These artifacts make cleaning difficult. In the shadow/sunlit contact, the points are higher than the rest of the points on the platform.

The 3D reconstruction obtained with ASP® was filtered (data deleted in post-processing with CloudCompare®) in the circles because of an unrealistic stair-step artifact. The 3D reconstruction from ERDAS IMAGINE® is not very dense within the circles, but the few scattered points allow realistic observation of the cliff foot (Figure 4).

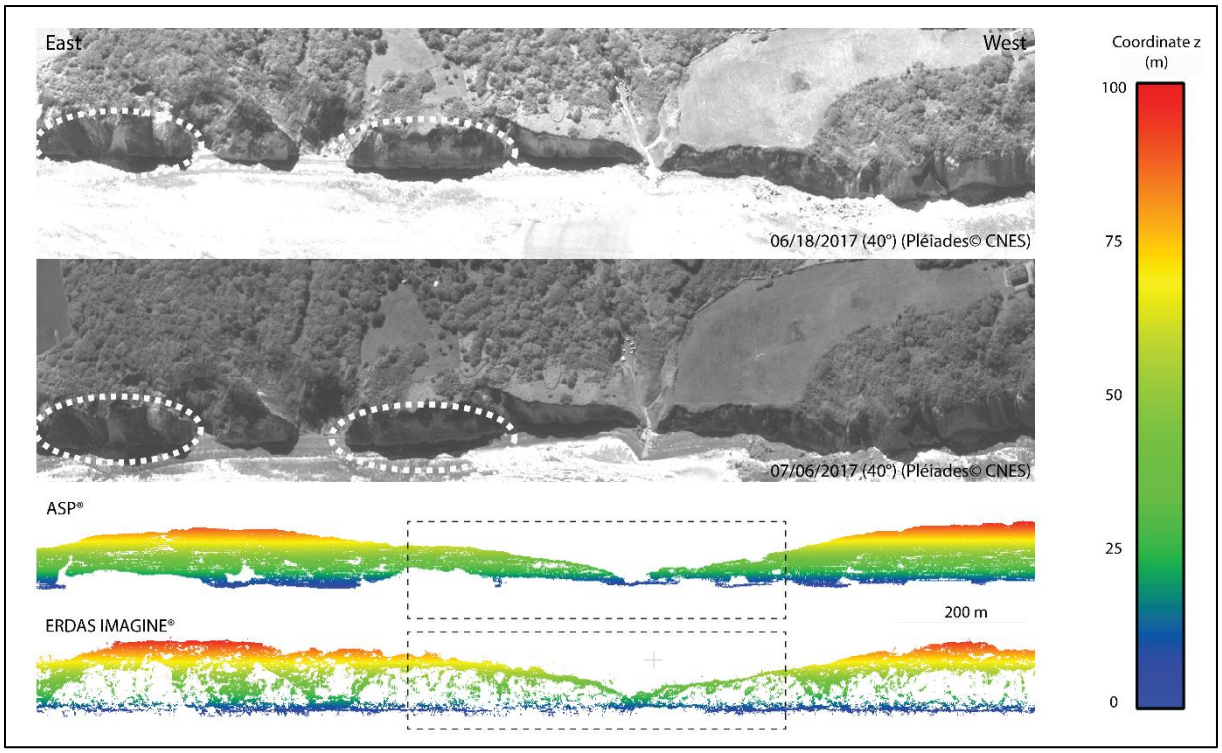

Figure 4: Distribution of points of the reconstructed cliff faces from the stereoscopic pair on 06/18/2017 and 07/06/2017 with a requested incidence angle of 40° at Varengeville-sur-Mer. The white dotted circles depict areas where the shadow/sunlit contact is located about 20 m from the foot of the cliff, thus where reconstruction is challenging.

4.1.3. Planimetric precision assessment

To georeference the point clouds from Pléiades images and compare them to multi-source data (UAV, TLS…), we proceeded to a semi-automatic co-registration using a rigid-body transform. This co-registration is efficiently constrained vertically (shore platform, plateau) and alongshore. Thus, precision error is assessed in the cross-shore direction (which is the direction of erosion on the cliff face).

The precision assessment is performed on the AOI of Varengeville-sur-Mer because UAV data were acquired on 06/26/2017 (by Azur Drones Company for RICOCHET research project). The precision assessment is based on the relative distance (normal of the cliff face) after fitting (Iterative Closest Point algorithm in Cloudcompare®) between the 3D point cloud reconstructed from Pléiades images (11 stereoscopic pairs in June and July 2017) and the one from UAV images (model). These synchronous surveys allow to limit errors due to erosion events. Table 5 summarizes the relative precision of the cliff face reconstructions.

Date of stereoscopic pairs		Requested incidence angle used for 3D reconstruction	Average relative distance (normal of cliff face) [standard deviation] with ASP®	Average relative distance (normal of cliff face) [standard deviation] with ERDAS IMAGINE®
06/10/2017	06/15/2017	0-10°	0.10 [4.94]	0.45. [2.69]
06/15/2017	07/06/2017	0-10°	0.05 [4.45]	0.06 [2.34]
06/10/2017	06/15/2017	40°	0.76 [3.88]	0.43 [3.04]
06/10/2017	06/18/2017	40°	0.26 [3.55]	0.83 [2.47]

06/10/2017	07/06/2017	40°	-0.23 [3.59]	0.00 [2.81]
06/15/2017	07/21/2017	40°	0.89 [4.99]	0.62 [2.85]
06/15/2017	06/18/2017	40°	-0.01 [4.02]	0.57 [2.44]
06/15/2017	07/06/2017	40°	0.17 [4.62]	-0.09 [2.11]
06/18/2017	07/06/2017	40°	1.03 [4.04]	0.25 [1.86]
06/18/2017	07/21/2017	40°	1.23 [4.65]	-0.37 [2.82]
07/06/2017	07/21/2017	40°	0.07 [3.89]	0.63 [2.39]
Average relative distance (normal of cliff face) for the 11 stereoscopic pairs [average standard deviation]			**0.39 [4.24]**	**0.31 [2.53]**

Table 5: Relative distance of cliff face normal at Varengeville-sur-Mer between 3D reconstruction from Pléiades images (stereoscopic pairs in June and July 2017) and the one from UAV images (06/26/2017)

The precision of the cliff face reconstruction is slightly better with ERDAS IMAGINE® than ASP® (average relative distance of 0.31 m and 0.39 m respectively). Furthermore, the standard deviations are lower with ERDAS IMAGINE® than with ASP® (average standard deviation of 2.53 and 4.24 m respectively). With a better average precision associated with a low error dispersion on the cliff face, the 3D reconstruction with ERDAS IMAGINE® provides a reliable dataset. Nevertheless, these better results in precision can partly originate from lower point density of the ERDAS® point clouds than of ASP® point clouds.

Regardless of the processing software used, the precision of the cliff face reconstruction is better for acquisitions with a 0-10° incidence angle than with a 40° angle. Indeed, low angles of incidence can limit distortions and inaccuracies of the RPC-based sensor orientation.

The spatial distribution of the relative distance between cliff face reconstruction and UAV data is different in function of the software (Figure 5). The 3D reconstruction obtained with ASP® creates a difference of more than 10 m at the foot of the cliff, where an artifact in the shape of a stair step appears because of the shadow. Concerning the 3D reconstruction obtained with ERDAS IMAGINE®, the large differences (greater than 6 m) are scarce and mainly randomly distributed over the whole cliff face. These artifacts can be removed by manual filtering.

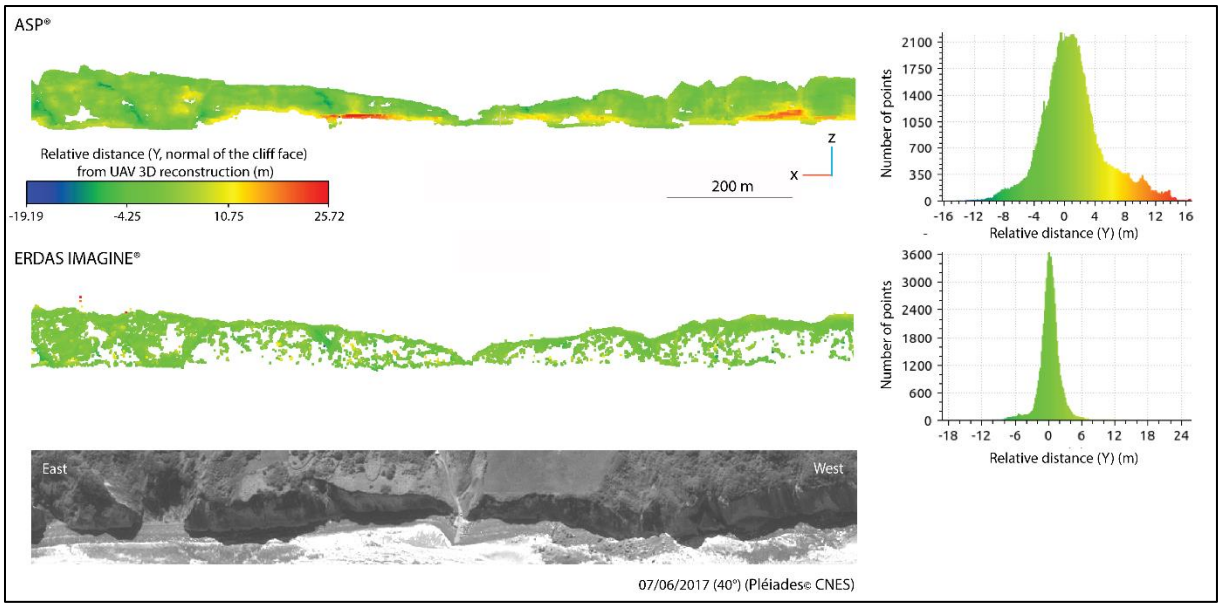

Figure 5: Relative distance of the cliff face normal (in m) at Varengeville-sur-Mer between 3D reconstructions with ERDAS IMAGINE® and ASP® (stereoscopic pair on 06/18/2017 and 07/06/2017 acquired at 40° requested incidence angle) in comparison with UAV data (06/26/2017)

In our study, despite a higher point density of the ASP® reconstruction compared to ERDAS IMAGINE® one, the latter software is more suitable because the reconstructed points are more precise and better distributed over the cliff face, providing a reliable dataset.

4.2. Identification of image pairs which give satisfactory reconstruction of the cliff face

First of all, the quality of 3D reconstruction of the cliff face proved to be less relevant than expected. Based on the point resolution on the cliff face, many couples have "unusable" reconstructions with very few points on the cliff face (< 1 pt/30 m) and/or with a proportion of computational artifacts greater than or equal to the proportion of valid points. Computational artifacts can be due to unsuitable geometry of acquisition between the images of the couple or bad tie point detection during correlation. Thus, for "usable" 3D reconstructions, less restrictive thresholds have been put in place:

- "few satisfactory" when the density is < 1 pt/15 m but a good signal to noise ratio;
- "satisfactory" when the density is > 1 pt/15 m (Figure 6).

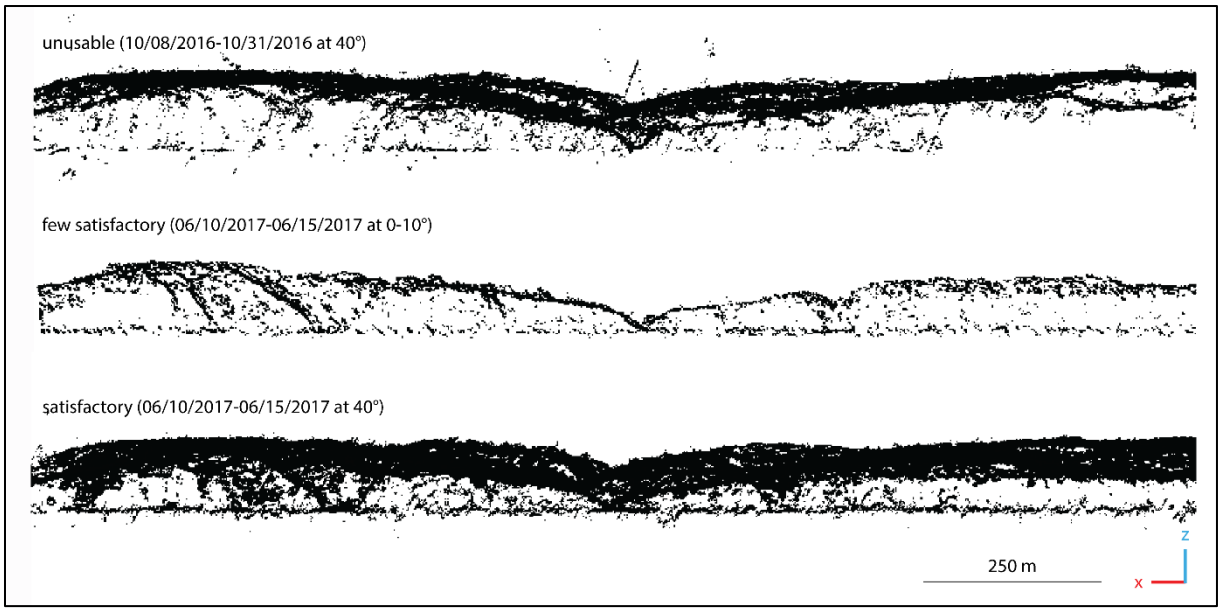

Figure 6: Ranking of 3D reconstruction quality of the cliff face in Varengeville-sur-Mer

The last threshold allows visibility of structural discontinuities from the cliff foot to the cliff top. Since ERDAS IMAGINE® creates reliable 3D reconstruction, this software is used to sort the different image pairs on the different AOI (Table 6).

Image 1	Image 2	Set of images (°)	Sainte-Marguerite-sur-Mer	Varengeville-sur-Mer	Dieppe	Puys
06/10/2017	06/15/2017	0-10	few satisfactory	few satisfactory	satisfactory	satisfactory
06/15/2017	07/06/2017	0-10	few satisfactory	satisfactory	satisfactory	satisfactory
12/01/2017	12/16/2017	0-10	unusable	unusable	unusable	unusable
01/24/2018	02/12/2018	0-10	unusable	unusable	unusable	few satisfactory
01/24/2018	02/17/2018	0-10	unusable	unusable	unusable	unusable
02/12/2018	02/17/2018	0-10	unusable	unusable	unusable	unusable
10/05/2016	10/08/2016	40	unusable	unusable	unusable	unusable
10/05/2016	10/31/2016	40	unusable	unusable	unusable	unusable
10/08/2016	10/31/2016	40	few satisfactory	unusable	unusable	unusable
06/10/2017	06/15/2017	40	few satisfactory	satisfactory	satisfactory	few satisfactory
06/10/2017	06/18/2017	40	satisfactory	satisfactory	satisfactory	satisfactory
06/10/2017	07/06/2017	40	few satisfactory	satisfactory	satisfactory	satisfactory
06/15/2017	06/18/2017	40	few satisfactory	satisfactory	satisfactory	few satisfactory
06/15/2017	07/21/2017	40	few satisfactory	satisfactory	unusable	unusable
06/15/2017	07/06/2017	40	satisfactory	satisfactory	satisfactory	satisfactory
06/18/2017	07/06/2017	40	few satisfactory	satisfactory	satisfactory	satisfactory
06/18/2017	07/21/2017	40	satisfactory	satisfactory	unusable	unusable
07/06/2017	07/21/2017	40	unusable	satisfactory	satisfactory	unusable
12/01/2017	12/16/2017	40	unusable	unusable	unusable	unusable

12/01/2017	01/24/2018	40	unusable	unusable	few satisfactory	unusable
01/24/2018	02/12/2018	40	unusable	unusable	unusable	unusable
01/24/2018	02/17/2018	40	unusable	unusable	satisfactory	unusable
02/12/2018	02/17/2018	40	unusable	unusable	unusable	unusable

Table 6: Quality of cliff face 3D reconstructions on ERDAS IMAGINE® in function of the 23 stereoscopic pairs

On the 92 tests, 29 give satisfactory 3D reconstruction (as in Figures 4 and 5), 13 are few satisfactory and the rest is unusable. Stereoscopic pairs at 40° provide more satisfactory 3D reconstruction over the four AOIs than stereoscopic pairs at 0-10°. Of the six stereoscopic pairs at 0-10°, two pairs give satisfactory results on two or three AOIs (mainly Dieppe and Puys). On 23 stereoscopic pairs at 40°, 10 pairs give satisfactory results, mainly on two areas of interest (Varengeville-sur-Mer and Dieppe). Two image pairs have satisfactory 3D reconstruction on the four AOIs: 06/10/2017-06/18/2017 and 06/15/2017-07/06/2017.

4.3. Identification of radiometric and geometric acquisition parameters favorable for 3D reconstruction of the cliff face

Unsurprisingly, the best images for cliff face reconstruction are those with:

- Sunny weather (e.g. 06/18/2017 and 07/06/2017 in Figures 4 and 5);
- Few shadows on the cliff face.

Both parameters are relevant for a satisfactory tie point detection because they provide various radiometric information. Over the four AOIs, the average radiometry of images which give satisfactory 3D reconstruction is between 300 and 400, whereas the standard deviation is between 80 and 94. This corresponds to a favorable ratio « mean/standard deviation » inferior to 5.

The main problem encountered in the 3D reconstruction is the cast shadow phenomenon on the cliff face (umbra and penumbra) that causes the partial or total loss of radiometric information (Arévalo et al., 2006). The summer season is the best period to limit this phenomenon, although it cannot be totally avoided because of the north-facing cliff along the studied coastline. Our current results mean that summer acquisitions are the most appropriate whereas a high temporal frequency is needed by scientists (from daily to seasonal surveys). In recent years several techniques have been studied to detect shadow areas and to compensate the loss of radiometric information or reconstruct it (for a review Shahtahmassebi et al., 2013; Al-Helaly and Muhsin, 2017). Shadow detection methods (thresholding, modeling, invariant color model, shade relief), and de-shadowing methods (e.g. visual analysis, mathematical models, fusion and data mining techniques) will be tested to improve radiometric information for better tie point detection and so higher quality 3D reconstruction.

For the geometric acquisition parameters, satisfactory reconstruction also comes from stereoscopic pairs at 0-10° but, with ERDAS IMAGINE®, the cliff face sampling distance is less satisfactory than for reconstruction from 40° stereoscopic pairs. However, the shortest distance between satellite/cliff face at 0-10° incidence angle than at 40° is prone to limited cloud cover. It may therefore be interesting to find a compromise between the incidence angle of images (from 10° to 40°) and the cliff face ground sampling. 3D cliff face reconstructions made by UAV images on the same study area show that 20°, 30° and 40° off-nadir imaging angles provide satisfactory results in terms of accuracy and texture restitution (Jaud et al., 2019). Therefore, a compromise with an angle of incidence of 20° seems promising and will be tested. Furthermore, because of the radiometric variations (different illumination conditions) and

geometric ones (in across-track direction) in multi-date stereoscopic pairs with the same incidence angle, it would be interesting to test 3D reconstruction from pairs of images acquired the same day at 0-10° and 40° (same radiometric configuration, but geometric variations in along-track direction).

4.4. Identification of site parameters most suitable for 3D reconstruction of the cliff face

The best reconstructed cliff faces are those in Dieppe and Varengeville-sur-Mer with 10 satisfactory 3D reconstructions (Table 6). This can be explained by the highest depths of incision (75 m at Dieppe and 115 m at Varengeville-sur-Mer) and the variability of the cliff face color (high standard deviations in radiometry, 103 and 124 at Varengeville-sur-Mer and Dieppe respectively) which allow easy detection of tie points due to texture change (Figure 4).

5. Conclusions

In this exploratory research, the potential of Pléiades satellite images to monitor coastal cliff face was investigated. The study area in Normandy (from Quiberville to Berneval-le-Grand) is particularly challenging because of its orientation (north-oriented cliff face) and the high frequency of cloud cover. To obtain images with high angle of incidence of the cliff face, a multi-date acquisition was specifically designed. The images with a high angle of incidence (from nadir to 40°) were processed using ASP® and ERDAS IMAGINE®. Interesting 3D reconstructions are obtained, especially with ERDAS IMAGINE® which provides more precise reconstructed points than ASP® (average relative distance and standard deviation of 0.31 m ± 2.53 and 0.39 m ± 4.24 respectively) and better distributed over the cliff face providing a reliable dataset. In our study, a minimum of 1 pt/15 m allows visibility of structural discontinuities from the cliff foot to the cliff top. Most of the satisfactory 3D point clouds come from stereoscopic pairs at 40° incidence angle and acquired in summer. The quality of 3D reconstruction of the cliff face mainly depends on radiometric quality, which is better with few cliff shadows and no cloud cover. Sites with deep incisions and cliff face color variability produce the best 3D reconstructions (Varengeville-sur-Mer and Dieppe). The potential of Pléiades images with high angle of incidence is interesting for 3D cliff face reconstruction in the study area if images are acquired in the summer. Because a high angle of incidence can be difficult to obtain from an image supplier, limiting the angle of incidence to about 20° may be a good compromise between the geometry of acquisition and the probability of cloud-free acquisition. This exploratory work creates numerous research opportunities. Seven prospects with Pléiades images will be tested soon: (1) 3D reconstruction with other software (e.g. MicMac®, S2P®, ENVI®) (2) de-shadowing methods over the Norman image dataset (3) multi-date tri-stereo reconstructions (4) a new approach to optimize 3D reconstruction on cliff face on specific areas where change is detected (5) 3D reconstruction from images acquired at the same date with both incidence angle (0-10° and 40°) (6) calculations of retreat distances and eroded volumes when the time interval between images is over 5 years (7) a new area with limited cloud cover, south-facing cliffs and images with an angle of incidence of 20°. For such applications, accurate detection and quantification of cliff face erosion require both a very high resolution and a pointing agility. Currently, WorldView (1 to 4) and Pléiades (1A and 1B) are the imagery satellites which best meet these needs, offering panchromatic Ground Sample Distance (GSD) lower or equal to 50 cm and pointing capability up to +/- 40°. The launching of Pléiades Neo constellation between 2020 and 2022 will also offer new opportunity.

Acknowledgments

The authors acknowledge financial support provided by the TOSCA project EROFALITT from the CNES (the French space agency). This work was also supported by ISblue project, Interdisciplinary graduate school for the blue planet (ANR-17-EURE-0015) and co-funded by a grant from the French government under the program "Investissements d'Avenir". This work was also supported by the ANR project “RICOCHET: multi-risk assessment on coastal territory in a global change context” funded by the French Research National Agency [ANR-16-CE03-0008]. This work is also part of the Service National d'Observation DYNALIT, via the research infrastructure ILICO.

The authors thank Scott McMichael, David Shean and Oleg Alexandrov, developers of the ASP® software at NASA, for quickly answering all questions about this software.

References

AIRBUS, 2015. Coastline Changes and Satellite Images Storms over La Salie Beach, French Atlantic Coast (Geo Reportage). AIRBUS Defence & Space.

Al-Helaly, E.A., Muhsin, I.J., 2017. A Review: Shadow Treatments and Uses Researches in Satellite Images. J. Kufa-Phys. 9, 20–31.

Almeida, L.P., Almar, R., Bergsma, E.W.J., Berthier, E., Baptista, P., Garel, E., Dada, O.A., Alves, B., 2019. Deriving High Spatial-Resolution Coastal Topography From Sub-meter Satellite Stereo Imagery. Remote Sens. 11, 590. https://doi.org/10.3390/rs11050590

Arévalo, V., González, J., Valdes, J., Ambrosio, G., 2006. Detecting shadows in QuickBird satellite images, in: ISPRS Commission VII Mid-Term Symposium" Remote Sensing: From Pixels to Processes", Enschede, the Netherlands. Citeseer, pp. 8–11.

ASTRIUM, 2012. Pléiades Imagery - User Guide (Technical report No. USRPHR-DT-125-SPOT-2.0).

Berthier, E., Vincent, C., Magnússon, E., Gunnlaugsson, á. þ., Pitte, P., Le Meur, E., Masiokas, M., Ruiz, L., Pálsson, F., Belart, J.M.C., Wagnon, P., 2014. Glacier topography and elevation changes derived from Pléiades sub-meter stereo images. The Cryosphere 8, 2275–2291. https://doi.org/10.5194/tc-8-2275-2014

Boak, E.H., Turner, I.L., 2005. Shoreline definition and detection: A review. J. Coast. Res. 21, 688–703. https://doi.org/10.2112/03-0071.1

Boissin, M.B., Gleyzes, A., Tinel, C., 2012. The pléiades system and data distribution, in: 2012 IEEE International Geoscience and Remote Sensing Symposium. Presented at the 2012 IEEE International Geoscience and Remote Sensing Symposium, pp. 7098–7101. https://doi.org/10.1109/IGARSS.2012.6352027

Collin, A., Hench, J.L., Pastol, Y., Planes, S., Thiault, L., Schmitt, R.J., Holbrook, S.J., Davies, N., Troyer, M., 2018. High resolution topobathymetry using a Pleiades-1 triplet: Moorea Island in 3D. Remote Sens. Environ. 208, 109–119. https://doi.org/10.1016/j.rse.2018.02.015

de Franchis, C., Meinhardt-Llopis, E., Michel, J., Morel, J.-M., Facciolo, G., 2014a. Automatic digital surface model generation from Pléiades stereo images. Rev. Fr. Photogrammétrie Télédétection 137–142.

de Franchis, C., Meinhardt-Llopis, E., Michel, J., Morel, J.-M., Facciolo, G., 2014b. On stereo-rectification of pushbroom images, in: Image Processing (ICIP), 2014 IEEE International Conference On. IEEE, pp. 5447–5451.

Gardel, A., Gratiot, N., 2006. Monitoring of coastal dynamics in French Guiana from 16 years of SPOT satellite images. J. Coast. Res. 1502–1505.

James, M.R., Robson, S., 2012. Straightforward reconstruction of 3D surfaces and topography with a camera: Accuracy and geoscience application. J. Geophys. Res. Earth Surf. 117. https://doi.org/10.1029/2011JF002289

Jaud, M., Letortu, P., Théry, C., Grandjean, P., Costa, S., Maquaire, O., Davidson, R., Le Dantec, N., 2019. UAV survey of a coastal cliff face - Selection of the best imaging angle. Measurement 139, 10–20. https://doi.org/10.1016/j.measurement.2019.02.024

Kennedy, D.M., Stephenson, W.J., Naylor, L.A., 2014. Rock coast geomorphology: A global synthesis, Geological Society. ed. Kennedy D.M., Stephenson W.J. and Naylor L.A., London.

Kotov, A.P., Goshin, Y.V., Gavrilov, A.V., Fursov, V.A., 2017. DEM generation based on RPC model using relative conforming estimate criterion. Procedia Eng. 201, 708–717.

Letortu, P., Costa, S., Bensaid, A., Cador, J.-M., Quénol, H., 2014. Vitesses et modalités de recul des falaises crayeuses de Haute-Normandie (France): méthodologie et variabilité du recul. Geomorphol. Relief Process. Environ. 20, 133–144. https://doi.org/10.4000/geomorphologie.10872

Letortu, P., Costa, S., Maquaire, O., Davidson, R., 2019. Marine and subaerial controls of coastal chalk cliff erosion in Normandy (France) based on a 7-year laser scanner monitoring. Geomorphology 335, 76–91. https://doi.org/10.1016/j.geomorph.2019.03.005

Letortu, P., Jaud, M., Grandjean, P., Ammann, J., Costa, S., Maquaire, O., Davidson, R., Le Dantec, N., Delacourt, C., 2018. Examining high-resolution survey methods for monitoring cliff erosion at an operational scale. GIScience Remote Sens. 55, 457–476. https://doi.org/10.1080/15481603.2017.1408931

Lim, M., Petley, D.N., Rosser, N.J., Allison, R.J., Long, A.J., Pybus, D., 2005. Combined digital photogrammetry and time-of-flight laser scanning for monitoring cliff evolution. Photogramm. Rec. 20, 109–129. https://doi.org/10.1111/j.1477-9730.2005.00315.x

Michoud, C., Carrea, D., Costa, S., Derron, M.H., Jaboyedoff, M., Delacourt, C., Maquaire, O., Letortu, P., Davidson, R., 2014. Landslide detection and monitoring capability of boat-based mobile laser scanning along Dieppe coastal cliffs, Normandy. Landslides 12, 403–418. https://doi.org/10.1007/s10346-014-0542-5

Mortimore, R.N., Stone, K.J., Lawrence, J., Duperret, A., 2004. Chalk physical properties and cliff instability, in: Coastal Chalk Cliff Instability, Geological Society Engineering Geology Special Publication. pp. 75–88.

Moses, C., Robinson, D., 2011. Chalk coast dynamics: Implications for understanding rock coast evolution. Earth-Sci. Rev. 109, 63–73. https://doi.org/10.1016/j.earscirev.2011.08.003

NASA, 2019. The Ames Stereo Pipeline: NASA's Open Source Automated Stereogrammetry Software (No. Version 2.6.2). NASA.

Naylor, L.A., Stephenson, W.J., Trenhaile, A.S., 2010. Rock coast geomorphology: Recent advances and future research directions. Geomorphology 114, 3–11. https://doi.org/10.1016/j.geomorph.2009.02.004

Neumann, B., Vafeidis, A.T., Zimmermann, J., Nicholls, R.J., 2015. Future Coastal Population Growth and Exposure to Sea-Level Rise and Coastal Flooding - A Global Assessment. PLOS ONE 10, e0118571. https://doi.org/10.1371/journal.pone.0118571

Pédelaborde, P., 1958. Le climat du Bassin Parisien : essai d'une méthode rationnelle de climatologie physique.

Poli, D., Remondino, F., Angiuli, E., Agugiaro, G., 2015. Radiometric and geometric evaluation of GeoEye-1, WorldView-2 and Pléiades-1A stereo images for 3D information extraction. ISPRS J. Photogramm. Remote Sens. 100, 35–47. https://doi.org/10.1016/j.isprsjprs.2014.04.007

Pomerol, B., Bailey, H.W., Monciardini, C., Mortimore, R.N., 1987. Lithostratigraphy and biostratigraphy of the Lewes and Seaford chalks: A link across the Anglo-Paris Basin at the Turonian-Senonian boundary. Cretac. Res. 8, 289–304.

Rupnik, E., Deseilligny, M.P., Delorme, A., Klinger, Y., 2016. Refined satellite image orientation in the free open-source photogrammetric tools APERO/MICMAC. ISPRS Ann. Photogramm. Remote Sens. Spat. Inf. Sci. 3, 83.

Salvini, R., Anselmi, M., Rindinella, A., Callegari, I., 2004. Quickbird stereo-photogrammetry for geological mapping (Cyrene-Libya), in: Proceedings of the 20th ISPRS Congress. Presented at the ISPRS Congress, Istanbul, Turkey, pp. 1101–1104.

Shahtahmassebi, A., Yang, N., Wang, K., Moore, N., Shen, Z., 2013. Review of shadow detection and de-shadowing methods in remote sensing. Chin. Geogr. Sci. 23, 403–420.

Shean, D.E., Alexandrov, O., Moratto, Z.M., Smith, B.E., Joughin, I.R., Porter, C., Morin, P., 2016. An automated, open-source pipeline for mass production of digital elevation models (DEMs) from very-high-resolution commercial stereo satellite imagery. ISPRS J. Photogramm. Remote Sens. 116, 101–117.

Stumpf, A., Malet, J.-P., Allemand, P., Ulrich, P., 2014. Surface reconstruction and landslide displacement measurements with Pléiades satellite images. ISPRS J. Photogramm. Remote Sens. 95, 1–12. https://doi.org/10.1016/j.isprsjprs.2014.05.008

Trzpit, J., 1970. Climat, in: Atlas de Normandie. p. 2.

Vanderstraete, T., Goossens, R., Ghabour, T.K., 2003. Bathymetric mapping of coral reefs in the Red Sea (Hurghada, Egypt) using Landsat7 ETM+ Data. Belgeo 3, 257–268.

Westoby, M.J., Lim, M., Hogg, M., Pound, M.J., Dunlop, L., Woodward, J., 2018. Cost-effective erosion monitoring of coastal cliffs. Coast. Eng. 138, 152–164. https://doi.org/10.1016/j.coastaleng.2018.04.008

White, K., El Asmar, H.M., 1999. Monitoring changing position of coastlines using Thematic Mapper imagery, an example from the Nile Delta. Geomorphology 29, 93–105. https://doi.org/10.1016/S0169-555X(99)00008-2

Young, A.P., 2018. Decadal-scale coastal cliff retreat in southern and central California. Geomorphology 300, 164–175. https://doi.org/10.1016/j.geomorph.2017.10.010

Young, A.P., Carilli, J.E., 2019. Global distribution of coastal cliffs. Earth Surf. Process. Landf. 44, 1309–1316. https://doi.org/10.1002/esp.4574